



Influence of Plasma Instabilities in Ceramic Suspension Plasma Spraying

R. Etchart-Salas, V. Rat, J.F. Coudert, P. Fauchais, N. Caron, K. Wittman, and S. Alexandre

(Submitted March 19, 2007; in revised form June 29, 2007)

Direct current Suspension Plasma Spraying (SPS) allows depositing finely structured coatings. This article presents an analysis of the influence of plasma instabilities on the yttria-stabilized suspension drops fragmentation. A particular attention is paid to the treatment of suspension jet or drops according to the importance of voltage fluctuations (linked to those of the arc root) and depending on the different spray parameters such as the plasma forming gas mixture composition and mass flow rate and the suspension momentum. By observing the suspension drops injection with a fast shutter camera and a laser flash sheet triggered by a defined transient voltage level of the plasma torch, the influence of plasma fluctuations on jet or drops fragmentation is studied through the deviation and dispersion trajectories of droplets within the plasma jet.

Keywords ceramic oxide layers, fuel cells, influence of spray parameters, nano-powders

1. Introduction

A relatively new process, Suspension Plasma Spraying (SPS), allows forming finely structured coatings rapidly and economically (Ref 1-3), using conventional spray installations where, instead of micron sized particles (about 20-80 μm) suspension drops or jet are injected. With this process, submicron solid particles, using a liquid feedstock carrier, can be sprayed onto a prepared substrate (Ref 4-6). When the suspension is injected into a Direct Current (D.C.) plasma jet at atmospheric pressure, first the liquid is fragmented into dispersed droplets a few microns in diameter, second the droplets of solvent are accelerated, vaporized, and transformed into plasma (Ref 2, 7), and finally the solid particles of the suspension contained within droplets are melted and again accelerated toward the substrate where they are flatten to form splats (Ref 8) at least for those, whose Stokes number is over 1. Due to the finer size of the powder injected, compared to conventional one, the coating thickness can

vary between a few tens of microns and a few hundreds of microns depending on spray conditions. Besides if, in conventional spraying, splats have diameters between 60 and 150 μm for zirconia with thickness between 0.8 and 2.5 μm , with the suspension spraying their diameters are below 3 μm and their thickness below 100 nm (Ref 3, 4) resulting in finely structured coatings.

Compared to conventional spraying where the arc fluctuations already have an important influence on particles velocities and temperatures, especially for those below 40 μm (Ref 9), with the suspension this influence is by far more important because fluctuations act on drops or jet penetration, fragmentation, particle trajectories, heating and acceleration. The fragmentation of the liquid jet is a very complex phenomenon which depends of the Weber number, $We = \rho_g U^2 d_s / \sigma$ (where, σ , ρ_g , d_s , and U are respectively, the surface tension of liquid (N/m^1), the plasma specific mass (kg/m^3), the diameter of the drop (m), and the relative velocity between the drop and the plasma (m/s^1)), which represents the ratio of the aerodynamic force to the surface tension force of the liquid. It is generally admitted that fragmentation takes place as soon as $We > 14$. Moreover, plasma properties (e.g., velocity, specific enthalpy, gas mass density) vary continuously along the plasma jet radius i.e., along the suspension penetration path toward the plasma jet axis. The instabilities of the arc root of the D.C. torch involve high transient voltage fluctuations and thus dissipated power fluctuations, resulting in plasma jets varying continuously in length and position (Ref 10) with strong variations of their velocities in the axial direction. Hence, materials (liquid or solid) embedded in the plasma flow undergo strong variations of the thermal and kinetic transfers. When the suspension drop penetration within the plasma jet is poor, the fragmentation is also poor and particles contained in resulting droplets undergo low thermal and kinetic transfers, thus impacting the substrate in a semimolten state, and increasing the porosity of the deposit if they stick to it.

This article is an invited paper selected from presentations at the 2007 International Thermal Spray Conference and has been expanded from the original presentation. It is simultaneously published in *Global Coating Solutions, Proceedings of the 2007 International Thermal Spray Conference*, Beijing, China, May 14-16, 2007, Basil R. Marple, Margaret M. Hyland, Yuk-Chiu Lau, Chang-Jiu Li, Rogerio S. Lima, and Ghislain Montavon, Ed., ASM International, Materials Park, OH, 2007.

R. Etchart-Salas, V. Rat, J.F. Coudert, and P. Fauchais, SPCTS, University of Limoges, Limoges Cedex, France; and **N. Caron, K. Wittman, and S. Alexandre**, DMA/SDI/LPTH, CEA Le Ripault, Monts, France. Contact e-mail: etchartsalas@yahoo.fr.

In conventional plasma spraying, Moreau et al. (Ref 9, 11) have shown that the arc root and corresponding power fluctuations have a drastic effect on in-flight alumina particle velocities and temperatures. When introducing suspensions of much smaller (0.1-1 μm) and lighter particles, is the effect of fluctuations enhanced or not? The aim of this article is to achieve a better understanding of the transient interaction between the suspension jet and the fluctuating plasma jet, in order to ensure the repeatability of coating properties (microstructural, electrical, and thermal). Hence, the injection of the suspension is observed with a fast shutter camera coupled to a laser flash sheet and triggered by a defined instantaneous voltage level of the plasma torch. Pictures taken with this device, allow observing the time-resolved suspension-plasma interaction for different torch working parameters.

First, the experimental facilities will be presented, then the plasma suspension interaction study, and at last the optimization of injection parameters.

2. Experimental Facilities

2.1 Injection System of the Suspension

The aim of this work is to adapt a new injection system to a commonly used plasma torch, namely a PTF4 which is available at the laboratory. The transverse injection outside of the nozzle was chosen, because previous works have shown that an internal transverse injection led to nozzle clogging. The injector system is composed of tanks in which the suspension is stored, and a stainless steel tube with its extremity a diaphragm on which a calibrated hole is machined (150 μm in these experiments). The suspension is counter-flow injected, with 10° angle with respect to the vertical axis at the nozzle exit at a distance of 23 mm from the torch axis and aiming the nozzle plane center. The injection velocity is adjusted by monitoring the tank pressure using compressed air. This system permits to work with drop injection velocities between 23 ± 2 m/s and 35.5 ± 2 m/s.

2.2 Plasma Torch

A commercial D.C. plasma torch (PTF4 from Sultz Metco) is used with an anode nozzle internal diameter of 6 mm. The working parameters of the torch (arc current intensity, voltage, thermal efficiency, and gas mass flow rate) are measured and recorded for each experiment, using a homemade computer code.

Experiments were started with the spray conditions used to spray conventional 22-45 μm YSZ (8 wt.%) powder with the PTF4 torch for thermal barrier coatings. Then, different plasma gas compositions were tested to reduce the level of fluctuations, level especially high with these conditions. Finally, the suspension tests were performed with the most characteristic mixtures: either Ar/H₂ (45/15 slm) or Ar/He (30/30 slm) mixtures. The Ar/H₂ plasma is generated with an arc current of 500 A, the voltage shows a mean value $\bar{V} = 60$ V, and fluctuations of

± 30 V, peak to peak corresponding to $\Delta V/\bar{V} = 1$. These arc instabilities, involve a high plasma jet fluctuation in length and position. The Ar/He plasma is generated with an arc current of 700 A. The replacement of hydrogen by helium and the increase of arc current allow reducing the mean voltage $\bar{V} = 40$ V and amplitudes of the voltage fluctuations $\Delta V = \pm 6$ V corresponding to, $\Delta V/\bar{V} = 0.3$.

2.3 Time-Resolved Imaging

The set up used to observe the suspension penetration within fluctuating plasma jets consists of a fast shutter camera coupled with a laser sheet flash at 808 nm. The image acquisition is triggered when the arc voltage reaches a given threshold. Therefore, the treatment of the material injected can be observed and correlated to an instantaneous state of the plasma flow. Figure 1 represents the time-resolved triggering of the system used. The arc voltage is recorded by a numerical oscilloscope and is sent to a triggering system which activates the camera. When the arc voltage reaches the chosen threshold, a voltage pulse activates the camera and after a factory set delay of 10-20 μs , the fast shutter opens. This delay is not adjustable, but correspond approximately to the time of flight of the plasma between the nozzle and the optical axis of the camera. With Ar-H₂ spray conditions the flow velocity at the nozzle exit (axis of the torch) varies roughly between 1000 and 2000 m/s during one period (200 μs) of the voltage fluctuation. Thus, 10 μs delay represents about 5% of the period time and that is why synchronization is never activated at the maximum of voltage fluctuations to avoid recording during the voltage drop. During the aperture of the shutter (10 μs), a laser shot (2 μs duration) is sent to illuminate the suspension jet, which otherwise is not sufficiently luminous compared to the plasma flame. The laser sheet thickness is about 1.5 mm and is focused to illuminate the plasma jet in order to see the liquid interaction with it. However, one problem is to illuminate the liquid jet, which, according to the injector vibrations, is not necessarily illuminated at each laser shot. All measurements (drop sizes and velocities) carried out by this optical system present an uncertainty of ± 1 pixel, the CCD matrix size being made of 400×480 pixels. According to the optic enlargement 1 pixel correspond to 30 μm . Thus drops or

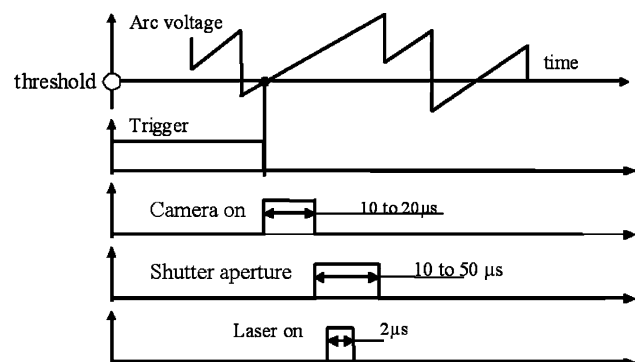


Fig. 1 Timing: Synchronization of the observational system

droplets over $30\ \mu\text{m}$ can be observed with a precision depending upon their size and below $30\ \mu\text{m}$ unfortunately the definition is not sufficient to observe details of fragmentation.

2.4 Liquid Jet Measurements

The suspension of Yttria-Stabilized Zirconia (YSZ) is made with a 7 wt.% powder dispersed within a solvent (ethanol), with a mass density of $860\ \text{kg/m}^3$. The stabilization and the dispersion of the suspension are ensured by a phosphate ester, whose percentage is adjusted to a previous study (Ref 4). The suspension jet shows weak instabilities within the first centimeters following the injector hole and is completely fragmented into drops after traveling a distance of $30 \pm 2\ \text{mm}$. The liquid jet before fragmentation is approximately $200 \pm 30\ \mu\text{m}$ in diameter and the drop mean diameter is about $290 \pm 30\ \mu\text{m}$. Therefore, it is possible to inject the suspension, either as a continuous jet or regular drops, depending on the distance between the injector tip and the torch axis. With a pressure tank of $4 \times 10^5\ \text{Pa}$, the drop velocity is $27 \pm 2\ \text{m/s}$, the mean distance between two consecutive drops is about $730 \pm 30\ \mu\text{m}$, and the number of drops emitted per unit times $3.7 \times 10^4/\text{s}$. In this condition, the liquid flow rate is of $0.47\ \text{cm}^3/\text{s}$.

3. Interaction Plasma/Suspension

3.1 High Fluctuation Level

The penetration of the suspension is first studied for the Ar/H₂ (45/15 slm) plasma gas, 503 A arc current, corresponds to the mean arc voltage of 60.6 V and torch thermal efficiency of 59%, parameters resulting in the specific enthalpy of 13.3 MJ/kg. Figure 2 represents the typical waveform of the arc voltage, with a period approximately equal to 200 μs .

The voltage fluctuation shape is linked to the geometry of the anode nozzle and that of the cathode together with the plasma forming gas composition. Moreover, on this wrapping of 200 μs , “restrike oscillations” of the arc root at higher frequencies can be identified. Therefore, the

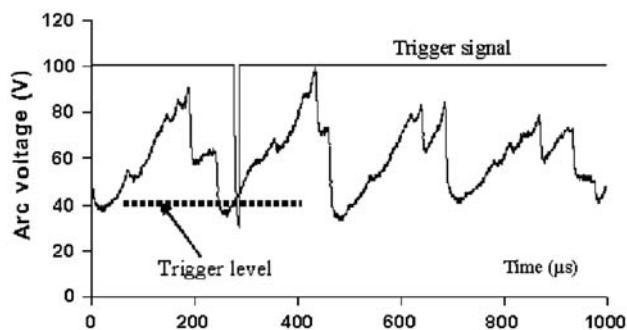


Fig. 2 Typical voltage waveform of an Ar/H₂ (45/15 slm) plasma gas (nozzle internal diameter 6 mm, $I = 503\ \text{A}$)

instantaneous electrical power supplied to the plasma gas is fluctuating in a frequency range of 2-10 kHz. The breakup mechanisms of the suspension drops, according to the continuous variation of the arc voltage, are observed thanks to the detection system triggered by a defined voltage level of the plasma torch. Figure 3 represents the fragmentation of the suspension for two different instantaneous plasma states.

The scale is given by the two horizontal dashed lines which are separated by the distance corresponding to the nozzle internal diameter (6 mm). Figure 3a shows the picture taken for an instantaneous arc voltage of 65 V. The distance between the injector tip and the torch axis is 23 mm; at that distance the liquid jet is not yet fragmented but shows weak instabilities whose wavelength is about 900 μm (see Fig. 3a). When the suspension jet penetrates the plasma and its fringes, it is broken at the neck of its own instabilities by the shear stress produced. Hence, several individual clouds of materials (liquid and/or solid) within the plasma jet can be clearly identified. These clouds are composed of a compact head of suspension and behind it, some sort of tail with tiny droplets and/or solid particles. The heads of the different clouds are equally spaced following the radius of the plasma, this distance being represented in the Fig. 3(a) by the horizontal white full lines. The distance along the liquid jet axis between two successive cloud heads correspond to the wavelength (900 μm) of the jet instabilities before entering the plasma. This means that the initial vertical velocity of the suspension ($26.6 \pm 2\ \text{m/s}$) is kept along the injection axis after its penetration within the jet (i.e., following plasma radius). Taking into account the velocity of the liquid, $26.6 \pm 2\ \text{m/s}$, the time required for traveling from the upper edge of the plasma jet down to its axis, 3 mm below, is approximately corresponding to the half period of the arc voltage fluctuations, that is about 100 μs . This “crossing time” is very important to understand the history of the heat and momentum transfer between the suspension and the plasma. Therefore, the cloud which travels toward the plasma jet axis is only treated by one puff of plasma, and the treatment of materials is strongly dependent on the properties of this puff (e.g., velocity and specific enthalpy).

The first comet (Fig. 3a), just under the upper edge of the plasma, enters into the jet approximately at the time at which the shutter is opened, which is also the time at which (within 10 μs) the arc voltage is 65 V in that particular case. Instead of that, the third comet, which is close to the plasma torch axis, has penetrated the jet about 60 μs earlier (Fig. 3a), when the voltage was about 40 V (see Fig. 2). During that time this cloud has covered an axial distance of 2 mm and is embedded in a region where the plasma shows a still high energy density. An estimation of the droplet velocities can be made by considering the fact that all the material belonging to the same cloud enters the plasma at the same time and also that the penetration of two consecutive drops are delayed by around 30 μs . As an example, considering the first and third comets in Fig. 3(a), it can be deduced that the axial distance covered by the head of one cloud is 1 mm during 60 μs , that gives around 17 m/s and, in the same time, that the top of the

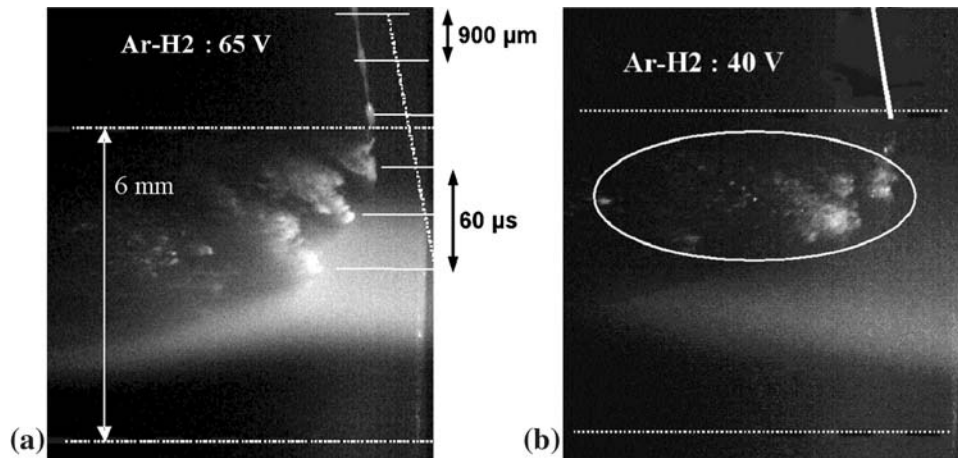


Fig. 3 Interaction plasma-suspension according to triggering level. Pictures according to triggering of Fig. 2 injection velocity of 26.6 m/s, and distance between the injector tip and torch axis 20 mm. (a) triggering level of 65 V, (b) triggering level of 40 V

tail is displaced over a three times longer distance, that gives around 50 m/s.

The picture of the Fig. 3(b) shows the interaction plasma-suspension with a low triggering level, namely 40 V. It is interesting to note that the liquid jet was insufficiently illuminated by the laser and thus not seen on the picture. In order to ease the understanding of the cloud treatments, the liquid jet has been represented by a white straight line. On the upper part of the plasma jet, the clouds originate from drops which have penetrated the plasma jet during a low voltage phase, showing a relatively low specific enthalpy and velocity. In this half period, the shear stress " $\rho_p u^2$ " applied to the suspension is lower than that of the preceding half period. But, in this picture no drops can be observed at the plasma jet axis position. This is due to the fact that the drops which are absent have penetrated into the plasma 100 μ s before this picture, was taken, i.e., during the preceding half period. This preceding period is characterized by higher mass enthalpy, temperature, and velocity. Thus, these clouds, which are absent, have been swept downstream by the preceding puff of plasma.

According to the high arc voltage fluctuations, each particle contained within the fragmented drops has its own thermal and kinetic histories which depends on the moment when it enters into the plasma. In order to reduce these arc root instabilities, an Ar/He mixture is tested thereafter.

3.2 Low Fluctuation Level

In order to homogenize the treatment of drops and then particles, the amplitude of plasma oscillations has to be reduced. Thus, the hydrogen has been replaced by helium and the arc current increased. In these conditions the "takeover mode" is favored, diminishing the arc voltage oscillations. The plasma is generated with 701 A arc current, and the flow rates of argon and helium are 30/30 slm. The torch thermal efficiency is 64%, the arc mean voltage is 39.9 V, and the specific enthalpy is 18.2 MJ/kg¹

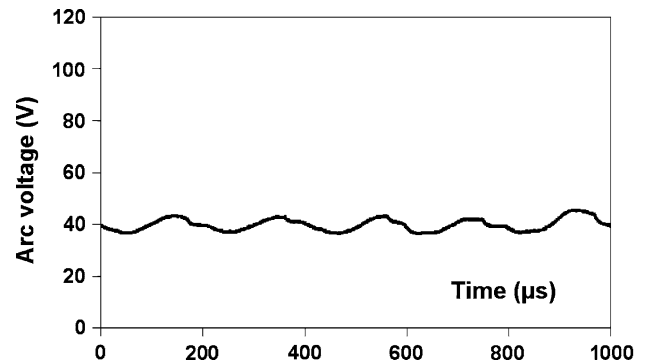


Fig. 4 Typical voltage waveform of an Ar/He (30/30 slm) plasma gas (nozzle diameter 6 mm, $I = 701$ A)

(higher than that with the Ar/H₂ mixture). The waveform of the arc voltage (Fig. 4) shows that the amplitude of the fluctuation has been reduced, nevertheless the wrap of fluctuation is still about 200 μ s. By the way this observation about the mean time of fluctuations supports the idea that these fluctuations depend strongly on the geometry of the nozzle and the electrode (Ref 12). Due to these weak fluctuations, no significant differences have been observed whatever was the triggering level. In Fig. 5, the liquid trajectory within the plasma flow is more homogeneous. Furthermore, with this relative steady plasma jet, the particle states at impact could be more easily homogenized.

Figure 5 shows that the liquid jet is fragmented into several clouds, as with a high plasma fluctuation level (see Fig. 3a). However, the different clouds within the plasma flow seem to occupy a region defined by two envelopes. The upper one corresponds to the extension of the comet tails, and near this envelope the flow is composed of tiny droplets and/or solid particles which are very sensitive to the plasma acceleration. Hence, this upper envelope delimits the high velocity of the materials into the plasma jet. On the contrary, the lower envelope is delimited by

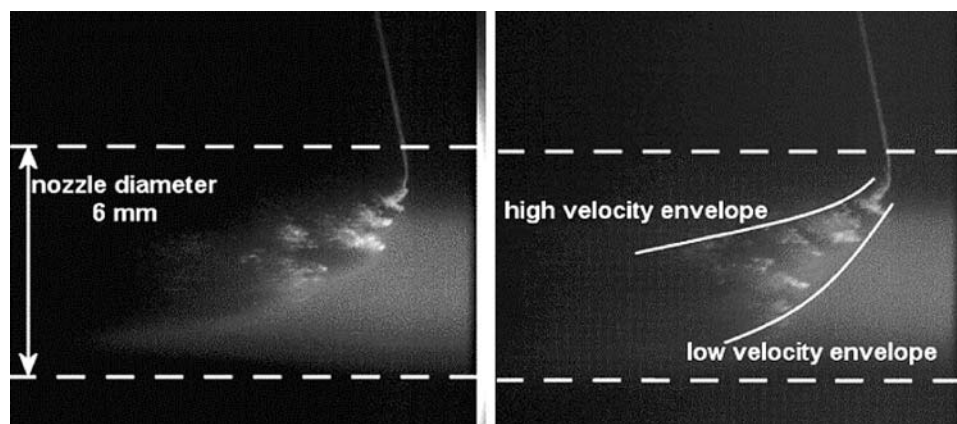


Fig. 5 Interaction plasma-suspension with the Ar/He plasma (working conditions of Fig. 4). Pictures whatever the triggering level, injection velocity of 26.6 m/s, and distance between the injector tip and the torch axis of 20 mm

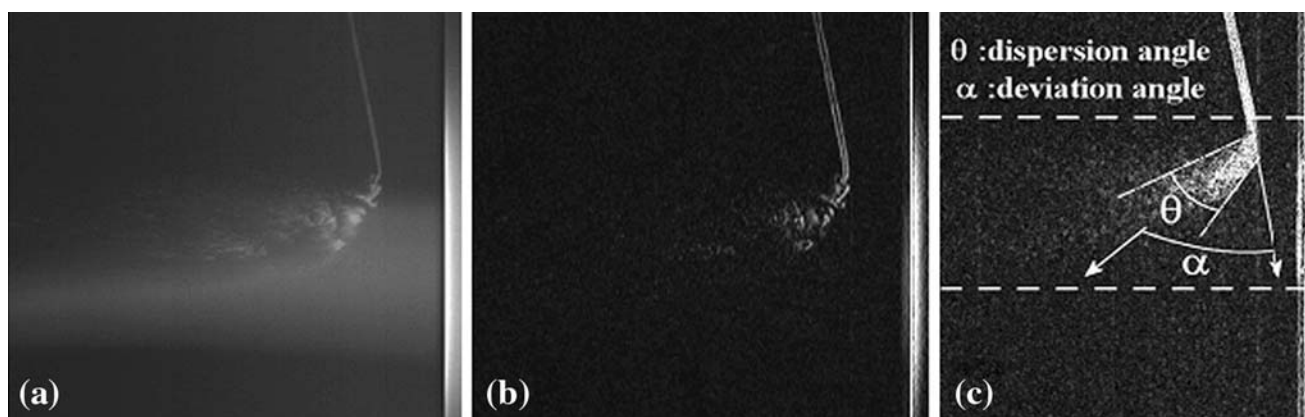


Fig. 6 Protocol of image processing: (a) original picture, (b) image obtained after the filtering, and (c) result of the sum of several images treated

the compact heads of the clouds, and characterized by the lower velocity of the droplets.

4. Optimization of Injection Parameters

4.1 Protocol of Image Processing

The preceding section has shown the importance of controlling the penetration and fragmentation of the suspension jet or drops into the fluctuating plasma. In order to ensure the quality and reproducibility of the coating formed in SPS, it is necessary to optimize the parameters which control drop trajectories. With the suspension itself, several parameters such as, the injection velocity, v , the surface tension force, σ , the mass density (load of powder), ρ , the internal diameter of the injector, and the suspension jet axis can be varied. The other group of adjustable parameters concerns the plasma torch working conditions, with the plasma forming gas composition and mass flow rate, the arc current intensity, and the

geometry of electrodes. The influence of the plasma gas mixture and the injection velocity are treated in this section. The other parameters have already been fixed (Ref 8).

The goal of this part is to superpose several images taken in the same conditions, in order to observe the mean trajectories of the materials within the plasma flow. However, if the different images are superposed, the weak luminosity of the liquid (Fig. 6a) is masked by the high one of plasma jet. Consequently, before superposing images, the first step, is to eliminate the plasma luminosity. Overlapped two filters (with matrox software) are applied on each image (Fig. 6b), a “median” filter, eliminating the noise of the picture, and a second filter, the “vertical edge,” allowing eliminating the plasma luminosity by the extraction of vertical contours. The liquid jet, as underlined previously, is not necessarily illuminated by the laser, thus when superposing images sometimes the liquid jet looks rather broad because of its uncontrolled vibrations or does not appear at all. In the latter case it has been represented by a white straight line.

Then, treated images taken in the same operating conditions are superposed (about 10), and in the final image (Fig. 6c) obtained, the cone of drops dispersion for fixed operating parameters can be observed. Starting from this final image (Fig. 6c), it is necessary to determine some parameters measurable in order to qualify the quality of the injection. Two parameters are chosen, the dispersion angle of the liquid within the plasma flow, θ , and the deviation angle of the suspension jet, α . The deviation angle, α , represents the mean penetration degree of the suspension into the plasma core. This deviation is proportional to the ratio of the quantity " $\rho_s v^2$ " (where, ρ_s is the suspension specific mass (kg/m^3), and v , the velocity of the jet (m/s)) of the suspension to that, " $\rho_p u^2$ " (where, ρ_p is the plasma specific mass (kg/m^3), and v , the velocity of the plasma jet (m/s)), of the plasma jet. The dispersion angle, θ , is representative of the homogeneity of the drops treatment. When the dispersion angle is large, the percentage of drops and then particles which travel near the plasma jet fringes increases. Thus, these particles have weaker thermal and kinetic transfers, and they impact the substrate under a semimolten state. Hence, a good injection of suspension is determined by a low cone of dispersion near the plasma jet axis. The different lines which allow measuring the dispersion and deviation angle are drawn manually (Fig. 6c). The angles are measured by image analyses with an accuracy of about 10-20%.

4.2 Influence of Plasma Gas Mixture

4.2.1 Argon-Hydrogen Plasma. The plasma generated is the Ar/H₂ (45/15 slm) with an arc current of 500 A, as in the preceding section. Therefore, the plasma presents high arc voltage fluctuations (Fig. 2). In Fig. 7(a), with high voltage, the materials occupy a region delimited by a dispersion cone of 33°, and the deviation angle of the suspension jet is 60.5°.

According to Fig. 7(b), corresponding to low voltage, the drops dispersion angle is very large, 64°, this is due to the drastic variation of plasma velocity between the consecutive half periods. Figure 7a shows that using

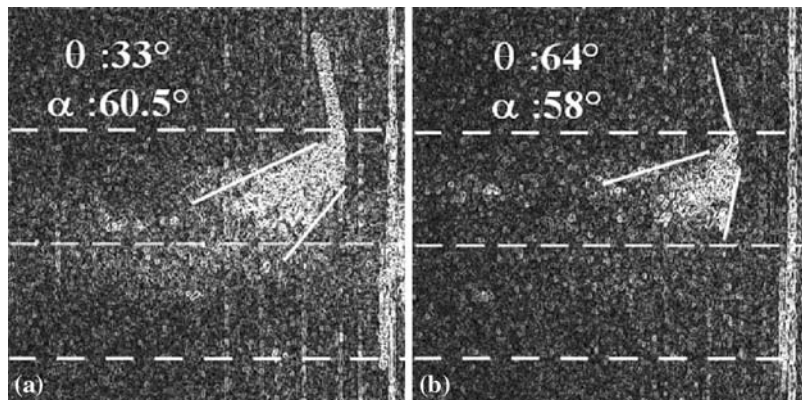


Fig. 7 Interaction plasma-suspension with an injection velocity of 26.6 m/s, distance between the injector tip and the torch axis of 20 mm: (a) high voltage level of Ar/H₂ plasma, (b) low voltage level of Ar/H₂ plasma (working conditions of Fig. 2)

Ar/H₂ plasma jet and suspension injected at 26.6 m/s, the drop trajectories are very different due to the arc instabilities. A fluctuating plasma flow induces strong variations of the dispersion cone; in these operating conditions particles which form the coating have undergone very different thermal and kinetic transfers according to their trajectories. However, the deviation angle does not present significant differences with the arc voltage level. Furthermore, no materials within the dispersion cone cross the plasma jet axis. Thus, the distribution of particles in the plasma cross section should be heterogeneous.

4.2.2 Argon-Helium Plasma. The Ar/He plasma gas is generated with an arc current of 700 A, in the same operating condition than those of Fig. 4. Different pictures of injection are taken whatever may be the triggering level, and Fig. 8 presents the result of images processing.

Using this relatively steady plasma jet, the dispersion angle is drastically reduced, 15°, against 64° with Ar/H₂. Figure 8 confirms the idea that the dispersion of particle trajectories, within the plasma, is directly dependent on

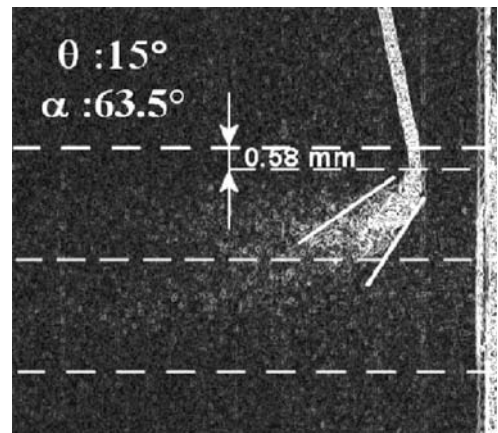
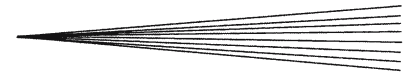


Fig. 8 Interaction plasma-suspension with an injection velocity of 26.6 m/s, distance between the injector tip and the torch axis of 20 mm, Ar/He plasma (working conditions of Fig. 4)



the torch voltage fluctuations. The deviation angle of the suspension with this Ar/He plasma is 63.5° , value slightly higher than that obtained with the Ar/H₂ plasma gas. However, it can be observed that the penetration depth of the suspension jet in the plasma jet fringes (determined by counting pixels), of 0.58 mm (see Fig. 8) is better. The suspension jet is apparently not fragmented into the cold boundary layer of the Ar/He plasma, thus involving that the fragmentation step and then the vaporization one occur closer to the plasma jet axis. Thus, it can be supposed that the melting and acceleration of particles are more homogeneously distributed in the plasma jet cross section.

4.3 Influence of the Injection Velocity

4.3.1 Argon-Hydrogen Plasma. In SPS, because of the fragmentation and the vaporization of the solvent, the quantity " $\rho_s v^2$ " of the suspension must be higher than that of plasma. But, the ratio between these two quantities which allows obtaining a good penetration is not clearly identified. Moreover, the " $\rho_s v^2$ " of the suspension decreases while approaching the plasma axis, and in the same time the shear stress applied by the plasma flow increases drastically. In this section two injection velocities are tested, 26.6 m/s using a pressure tank of 0.4 MPa, and 33.5 m/s for a pressure tank of 0.6 MPa. Figure 9a shows

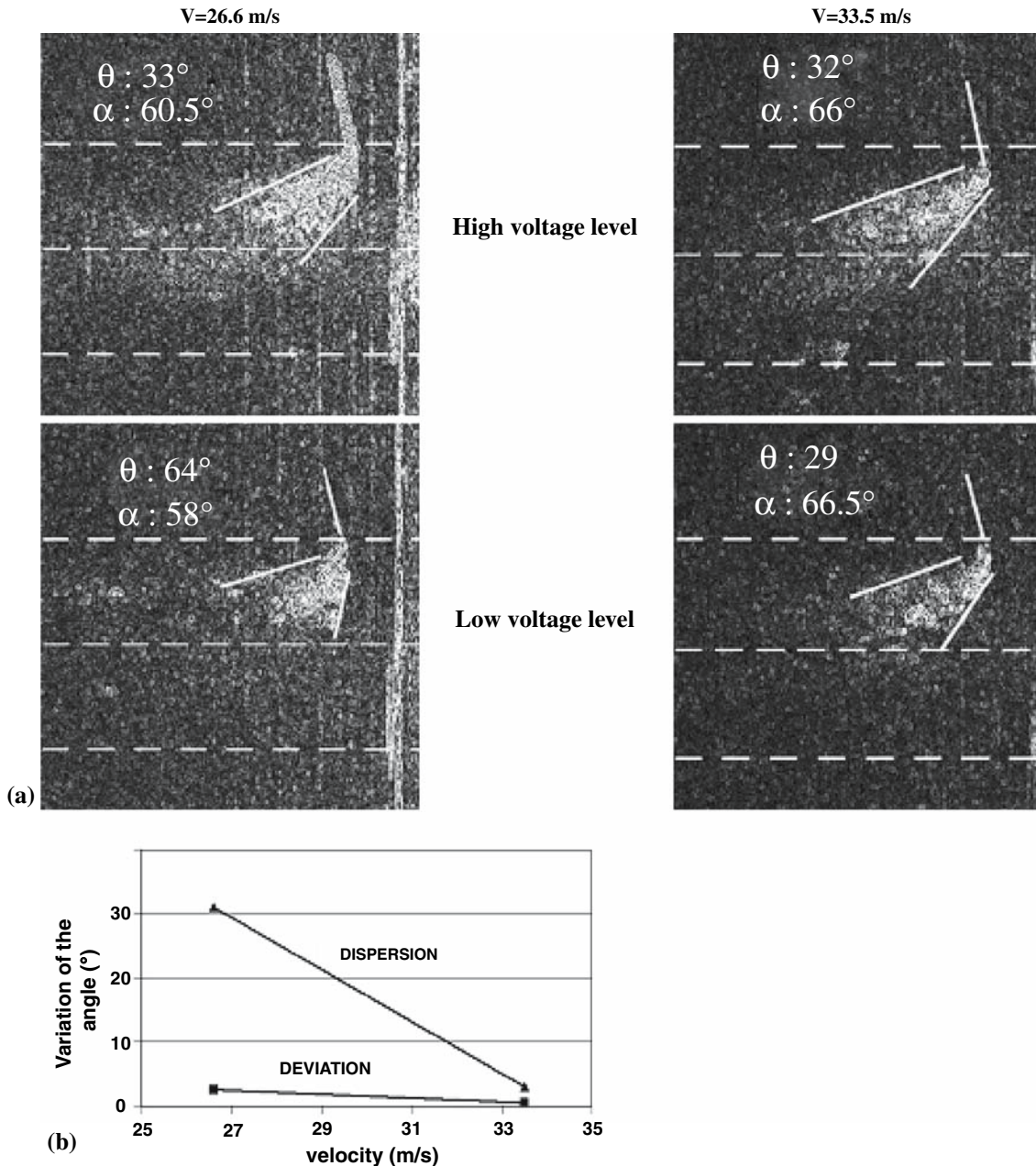


Fig. 9 Evolution of the interaction plasma-suspension with the suspension injection velocity using an Ar/H₂ plasma (working conditions of Fig. 2)

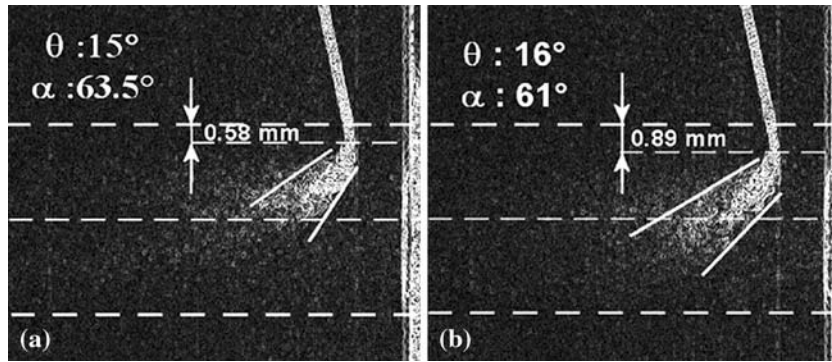


Fig. 10 Evolution of the interaction plasma-suspension with the injection velocity using an Ar/He plasma (working conditions of Fig. 4): (a) injection velocity, 26.6 m/s and (b) injection velocity, 33.5 m/s

two different behaviors depending on the velocity of the suspension jet injected.

The dispersion angle for a low voltage level has diminished from 64° to 29° as the injection velocity increases. Thus, the enhancement of the velocity decreases the variation of the angle dispersion whatever may be the triggering level. With the high velocity, 33.5 m/s, the cone of dispersed particles is closer to the plasma jet axis, where the shear stress increases, hence the deviation angle is the highest in these conditions: 66° . The graph in the Fig. 9(b) presents the variation of the different angles according to the injection velocity. As the variation of the two angles diminishes, it can be concluded that the injection is stabilized with a suspension jet velocity of 33.5 m/s. With the suspension jet velocity of 26.6 m/s the quantity “ $\rho_s v^2$ ” is 0.61 MPa, while with the highest velocity (33.5 m/s), this quantity increases by 60% (0.96 MPa). The mean velocity, u , of the Ar/H₂ plasma is dependent on the arc voltage of the torch (Ref 13):

$$u \propto \frac{\eta I}{p_a \cdot \pi \cdot r^2} \cdot \frac{\gamma - 1}{\gamma} \cdot U$$

where, u , γ , d , p_a , U , and η are respectively, the plasma velocity (m/s), isentropic coefficient (-), the nozzle internal diameter (m), atmospheric pressure (Pa), the arc voltage (V), and torch thermal efficiency (-).

The arc voltage, V , shows important time variations (40-100 V) with argon-hydrogen plasma (Fig. 2). In the plasma the quantity “ $\rho_p u$ ” is almost constant (Ref 8), thus, the shear stress ($\rho_p u^2$) applied by the plasma varies as its velocity linked to arc voltage. Furthermore, the quantity of 0.61 MPa (low velocity: 26.6 ± 2 m/s) of the suspension is probably not sufficiently high to permit the good penetration of the liquid jet when the arc voltage is 100 V. Then in the next puff (40 V) drops near the top of the plasma jet are observed, which did not penetrate during the preceding period, and correlatively the dispersion angle increases (θ : 64° in Fig. 9).

4.3.2 Argon-Helium Plasma. Using the Ar/He plasma flow, the arc level voltage variations (Fig. 4) are drastically reduced ($\Delta V = 6$ V), and the mean voltage value is quasi constant, 40 V. Thus, the time-averaged plasma velocity is

constant. Figure 10 presents the evolution of the material trajectories within the Ar/He plasma flow.

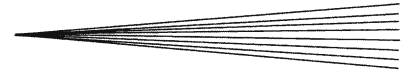
The angle of dispersion is always constant, thus whatever may be the injection velocity the trajectories of the drops are homogeneous. However, with the high injection velocity, the suspension jet is fragmented closer to the torch axis (Fig. 10b). In this case, the percentage of particles crossing the plasma jet axis increases to the detriment of particles which travel into the plasma jet fringes. Thus, the distribution of particles into the plasma jet cross section is more homogeneous.

5. Conclusion

The injection of suspension drops has been observed with a fast shutter camera coupled with a laser sheet flash, and triggered by a defined transient voltage level of the plasma torch. This study has shown that the plasma jet fluctuations have a strong influence on drops fragmentation. An important difference in drop trajectories within the plasma flow has been observed between the argon-hydrogen and argon-helium plasmas. This heterogeneity of drops treatment is due to arc voltage fluctuations. Image processing has allowed choosing some spray parameters in order to homogenize drop trajectories. The stabilization of the interaction plasma jet-zirconia suspension increases when using plasmas with low arc voltage oscillations. The suspension injection parameters (jet velocity) have to be adjusted according to plasma forming gases. Work is in progress to study coatings formed using the best spray parameters resulting from this study in order to validate it.

References

1. J. Oberste-Berghaus, B. Marple, and C. Moreau, Suspension Plasma Spraying of Nanostructured WC-12Co Coatings, *J. Thermal Spray Technol.*, 2006, **15**(4), p 676-681
2. R. Siegert, J.-E. Doring, J.-L. Marqués, R. Vaseen, D. Sebold, and D. Stöver, Denser Ceramic Coatings Obtained by the Optimisation of the Suspension Plasma Spraying Technique, *Proceedings of the ITSC 2004*, DVS, Düsseldorf, Germany, 2004, e-proceedings



3. P. Fauchais, R. Etchart-Salas, C. Delbos, M. Tognovi, V. Rat, J.F. Coudert, and T. Chartier, Suspension and Solution Plasma Spraying of Finely Structured Coatings, *J. Phys. D: Appl. Phys.*, 2007, **40**, p 1-13
4. P. Fauchais, V. Rat, C. Delbos, J. Fazilleau, J.F. Coudert, T. Chartier, and L. Bianchi, Understanding of Suspension Plasma Spraying of Finely Structured Coatings for SOFC, *IEEE Trans. Plasma Sci.*, 2005, **33**(2), p 920-930
5. P. Blazell and S. Kuroda, Plasma Spraying of Submicron Ceramic Suspensions Using a Continuous Ink Jet Printer, *Surf. Coat. Technol.*, 2000, **123**, p 239-246
6. R. Siegert, J.-E. Döring, J.-L. Marqués, R. Vassen, D. Sebold, and D. Stöver, Influence of the Injection Parameters on the Suspension Plasma Spraying Coating Properties, *Proceedings of the ITSC 2005*, DVS, Düsseldorf, Germany, 2005, e-proceedings
7. C. Delbos, V. Rat, C. Bonhomme, J. Fazilleau, J.F. Coudert, and P. Fauchais, Influence of Powder Size Distributions on Microstructural Features of Finely Structured Plasma Sprayed Coatings, *J. High Temp. Mater. Proc.*, 2004, **8**(3), p 397-407
8. C. Delbos, J. Fazilleau, V. Rat, J.F. Coudert, P. Fauchais, and B. Pateyron, Phenomena Involved in Suspension Plasma Spraying Part 2: Zirconia Particle Treatment and Coating Formation, *Plasma Chem. Plasma Process.*, 2006, **26**(4), p 493-414
9. C. Moreau, J.-F. Bisson, R.S. Lima, and B.R. Marple, Diagnostics for Advanced Materials Processing by Plasma Spraying, *Pure Appl. Chem.*, 2005, **77**(2), p 443-462
10. J.F. Coudert, M.P. Planche, and P. Fauchais, Characterization of D.C. Plasma Torch Voltage Fluctuations, *Plasma Chem. Plasma Process.*, 1996, **16**(1), p 211-227
11. C. Moreau, Advanced Particle Diagnostics for Controlling Plasma Spray Process, *Sensors and Control 2004*, ASM International, Materials Park, OH, USA, 2004, e-proceedings
12. E. Noguez, P. Fauchais, M. Vardelle, and P. Granger, Relation Between the Arc Root Fluctuations, the Cold Boundary Layer Thickness and the Particle Thermal Treatment, *Proceedings of the ITSC 2007*, DVS, Düsseldorf, Germany, 2007, e-proceedings
13. V. Rat and J.F. Coudert, A Simplified Analytical Model for dc Plasma Spray Torch: Influence of Gas Properties and Experimental Conditions, *J. Phys. D: Appl. Phys.*, 2006, **39**, p 4799-4807